[CANCER RESEARCH 64, 8541–8549, December 1, 2004]

Array Comparative Genomic Hybridization Analysis of Genomic Alterations in Breast Cancer Subtypes

Lenora W. M. Loo,[1,2] Douglas I. Grove,[2] Eleanor M. Williams,[1] Cassandra L. Neal,[3] Laura A. Cousens,[1,2] Elizabeth L. Schubert,[1,2] Ilona N. Holcomb,[1] Hillary F. Massa,[1] Jeri Glogovac,[1,2] Christopher I. Li,[2] Kathleen E. Malone,[2] Janet R. Daling,[2] Jeffrey J. Delrow,[3] Barbara J. Trask,[1] Li Hsu,[2] and Peggy L. Porter[1,2]

[1]Division of Human Biology, [2]Division of Public Health Sciences, and [3]Genomics Shared Resource, Fred Hutchinson Cancer Research Center, Seattle, Washington

ABSTRACT

In this study, we performed high-resolution array comparative genomic hybridization with an array of 4153 bacterial artificial chromosome clones to assess copy number changes in 44 archival breast cancers. The tumors were flow sorted to exclude non-tumor DNA and increase our ability to detect gene copy number changes. In these tumors, losses were more frequent than gains, and gains in 1q and loss in 16q were the most frequent alterations. We compared gene copy number changes in the tumors based on histologic subtype and estrogen receptor (ER) status, *i.e.,* ER-negative infiltrating ductal carcinoma, ER-positive infiltrating ductal carcinoma, and ER-positive infiltrating lobular carcinoma. We observed a consistent association between loss in regions of 5q and ER-negative infiltrating ductal carcinoma, as well as more frequent loss in 4p16, 8p23, 8p21, 10q25, and 17p11.2 in ER-negative infiltrating ductal carcinoma compared with ER-positive infiltrating ductal carcinoma (adjusted *P* values ≤ 0.05). We also observed high-level amplifications in ER-negative infiltrating ductal carcinoma in regions of 8q24 and 17q12 encompassing the *c-myc* and *c-erbB-2* genes and apparent homozygous deletions in 3p21, 5q33, 8p23, 8p21, 9q34, 16q24, and 19q13. ER-positive infiltrating ductal carcinoma showed a higher frequency of gain in 16p13 and loss in 16q21 than ER-negative infiltrating ductal carcinoma. Correlation analysis highlighted regions of change commonly seen together in ER-negative infiltrating ductal carcinoma. ER-positive infiltrating lobular carcinoma differed from ER-positive infiltrating ductal carcinoma in the frequency of gain in 1q and loss in 11q and showed high-level amplifications in 1q32, 8p23, 11q13, and 11q14. These results indicate that array comparative genomic hybridization can identify significant differences in the genomic alterations between subtypes of breast cancer.

INTRODUCTION

Conventional comparative genomic hybridization has been used to demonstrate chromosomal loss and gain in breast cancer (1, 2). However, resolution of conventional comparative genomic hybridization is limiting, and arrays of bacterial artificial chromosome (BAC) clones provide higher resolution comparative genomic hybridization for more accurate mapping of regions that contain oncogenes or tumor suppressor genes (3). Array comparative genomic hybridization (with BAC and cDNA arrays) has been used to localize copy number changes associated with human breast (4–6), prostate (7, 8), bladder (9), and gastric cancers (10). Recently developed DNA microarrays of overlapping clones increase the resolution of array comparative genomic hybridization to submegabase levels (11).

The use of conventional and array comparative genomic hybridization for the study of breast cancer is well established, and regions of frequent loss (6q, 13q, 16q, 17p, and 22q) and gain (1q, 6p, 8q, 11q, 16p, 17q, 19, and 20q) have been identified (1–3, 12–18). However, different etiologies and pathways are likely to be involved in the development of subtypes of breast tumors. Identification of alterations associated with tumor phenotypes, such as histologic type or steroid receptor expression, could provide information that is obscured when breast cancers of all types are analyzed together.

Steroid receptor status is one of the main differentiating characteristics of breast cancer. Estrogen receptor (ER)-negative tumors are more aggressive than ER-positive tumors, and the loss of ERs in tumor cells is associated with poor prognosis and poor response to hormonal therapy (19). Gene expression profiling identifies ERs as a fundamental classifier of breast cancers (20), suggesting that a molecular profile could define a set of alterations associated with aggressive breast cancer.

Similarly, the major histologic types of breast cancer, infiltrating ductal carcinoma and infiltrating lobular carcinoma, differ fundamentally. Infiltrating lobular carcinoma is more likely than the more common infiltrating ductal carcinoma to be steroid hormone receptor positive, diploid, bilateral, and multicentric, and to metastasize to bone (21, 22). Infiltrating lobular carcinoma tumors are associated with loss of E-cadherin protein expression through promoter methylation, mutation, and allelic loss (23) and exhibit more frequent genomic loss in 16q, 18q12-q21, 17q, and 22q than infiltrating ductal carcinoma (2, 13, 24).

In this study, we used array comparative genomic hybridization to assess gene copy number changes in 44 archival breast cancers chosen to represent lobular and ductal histologic types and ER-negative and ER-positive disease. We flow cytometrically sorted the tumors to exclude non-tumor DNA from analysis and increase our ability to identify gene copy loss. Array data were analyzed to determine chromosomal regions that might differentiate these important subtypes of breast cancer.

MATERIALS AND METHODS

Tumor Specimens. The 44 primary breast tumors were from women ages 36 to 74 years (mean = 59 years), identified through the Surveillance, Epidemiology, and End Results registry, diagnosed with invasive breast cancer between 1994 and 2001, and enrolled in ongoing epidemiologic studies at the Fred Hutchinson Cancer Research Center (Table 1). All tumors were reviewed for histologic grade and subtype (by P. Porter), evaluated for expression of ER and progesterone receptor (PR), c-erbB-2, and Ki-67 expression by immunohistochemistry, and assessed for DNA content by flow cytometry.

Flow Cytometry Cell Sorting. To restrict the inclusion of non-tumor cells from analysis, formalin-fixed, paraffin-embedded tumor samples were sorted by flow cytometry with a cytokeratin label as described previously (25). Briefly, thick sections of tumor samples were dissected to exclude normal breast epithelium, digested to prepare a cell suspension, and sorted by bivariate analysis based on cytokeratin expression and DNA content with 4′,6-diamidino-2-phenylindole fluorescence. This resulted in >90% purity of tumor cells in the sorted sample (25).

Received 6/8/04; revised 8/16/04; accepted 10/1/04.

Grant support: Department of Defense Grant DAMD 17-02-1-0386, National Cancer Institute Grant RO1 CA95717, and the Avon Foundation (P. Porter); National Cancer Institute Grant U24 CA80295 (B. Trask); National Cancer Institute Grant P50 CA97186, Department of Defense Grant DAMD 17-03-2-0033, and National Institute on Aging Grant RO1 AG14358 (L. Hsu); and National Cancer Institute Grants P30 CA15704-30, RO1 CA85913, NO1-HD2-3166 (J. Daling).

The costs of publication of this article were defrayed in part by the payment of page charges. This article must therefore be hereby marked *advertisement* in accordance with 18 U.S.C. Section 1734 solely to indicate this fact.

Requests for reprints: Peggy L. Porter, Division of Human Biology, Fred Hutchinson Cancer Research Center, 1100 Fairview Avenue North, Seattle, WA 98109-1024. Phone: (206) 667-3751; Fax: (206) 667-5815; E-mail: pporter@fhcrc.org.

Table 1 *Characteristics of 44 invasive breast tumors*

	Infiltrating ductal carcinoma		Infiltrating lobular carcinoma	
	No. of ER positive (%) 14 (32)	No. of ER negative (%) 13 (30)	No. of ER positive (%) 15 (34)	No. of ER negative (%) 2 (4)
Mean age at diagnosis (y)	62	54	60	57
Progesterone receptor				
Positive	14 (100)	5 (38)	12 (80)	0
Negative	0	8 (62)	3 (20)	2 (100)
c-erbB-2				
2–3+	0	5 (38)	0	1 (50)
neg-1+	14 (100)	8 (62)	15 (100)	1 (50)
DNA content by flow cytometry				
Diploid	9 (64)	4 (31)	12 (80)	0
Aneuploid	5 (36)	9 (69)	3 (20)	2 (100)
Histologic grade				
High	2 (14)	5 (38)	1 (7)	1 (50)
Intermediate	6 (43)	7 (54)	9 (60)	1 (50)
Low	6 (43)	1 (8)	5 (33)	0
Stage *				
Local	9 (64)	5 (38)	11 (73)	0
Regional	5 (36)	6 (46)	4 (27)	2 (100)
Distant	0	2 (15)	0	0

* Stage based on data from Surveillance, Epidemiology, and End Results.

DNA Extraction and Labeling. DNA was extracted from flow-sorted tumor cells (between 14,000 and 500,000 cells per tumor) as reported previously (26). Briefly, cells were incubated in 200 ng/μL proteinase K in 50 mmol/L Tris (pH 8.3) overnight at 37°C. Samples were boiled for 8 minutes to inactivate the proteinase K. Tumor DNA was quantified with PicoGreen dsDNA Quantitation kit (Molecular Probes, Eugene, OR). Normal female reference DNA was extracted with the QIAamp Blood Extraction Kit (Qiagen, Valencia, CA).

Normal reference DNA was digested with *Dpn*II and applied to a MinElute Reaction Clean-Up column (Qiagen). Random amplification and labeling steps were performed according to the method of Lieb, with modifications (27).[4] Briefly, a primer (primer A; 5′-GTTTCCCAGTCACGATCNNNNNNNNN-3′) containing a degenerate 3′-end and a specific 5′-end was randomly annealed to DNA templates (10 ng) and extended with a T7 polymerase (Sequenase Version 2.0, USB, Cleveland, OH). Then, a Cy3- or Cy5-labeled primer (5′-GTTTCCCAGTCACGATC-3′; Operon, Alameda, CA) specific to the 5′-end of primer A was used to PCR amplify the templates generated in the first reaction. PCR reactions were applied to a QIAquick PCR Purification column (Qiagen), blocking agents added (50 μg of human Cot-1 DNA and 100 μg of yeast tRNA; Invitrogen, Carlsbad, CA), concentrated with a Microcon 10 filter (Millipore, Bedford, MA), and pooled and dried.

Bacterial Artificial Chromosome Array. The BAC clones comprising the array are a subset of those described by the BAC Resource Consortium (28), augmented with clones containing genes relevant to tumorigenesis and single-copy clones lying near most chromosomal ends (29). Some sequence has been determined from each clone so that each clone could be positioned within the April 2003 human draft sequence (30).[5] Clones were positioned with their coordinate midpoints, except if a clone was placed by a single BAC end, in which case the midpoint was estimated to be 75 kb from the BAC end in the appropriate direction. BACs placed by sequence-tagged site are approximate but not off by ≥80 kb. Clones that were hybridized by fluorescence *in situ* hybridization to multiple chromosomal locations or to a cytogenetic location inconsistent with their position in the sequence assembly were excluded from analysis (28). Clones were also excluded based on criteria specified in the preprocessing step (below). A total of 4153 different BAC clones were used in the final analysis. The median spacing of the clones is 413 kb when pericentric heterochromatic regions and the short arms of acrocentric chromosomes are excluded (25th percentile, 160 kb; 75th percentile, 878 kb; mean, 677 kb). Y-Chromosome clones were not used. The locations of 89% of the 4153 clones were verified by fluorescence *in situ* hybridization. The list of 4153 clones and details about their coordinates in the April 2003 draft assembly is available online.[6] The clones are available from CHORI.[7]

Each of the 4153 BACs defines a domain in the genome: the region starting from the end position of the previous nonoverlapping clone on the array to the start position of the next nonoverlapping array clone. These domains were defined because any deletion or amplification seen in a clone can extend beyond the clone, and the extent is determined by the next unaffected clone on the array in either direction.

To construct the array, BAC DNA was extracted from 1.5-mL cultures with a modified Qiagen R.E.A.L. Prep96 plasmid kit (Qiagen). Purified BAC DNA was then amplified with ligation-mediated PCR (31) and cleaned with the Multiscreen-PCR filtration system (Millipore) on a Biomek FX automated liquid handling system (Beckman Coulter, Fullerton, CA). Purified products were transferred to 384-well plates, air-dried, and then resuspended in 3× SSC. Each amplified/purified BAC was then mechanically spotted in triplicate onto poly-L-lysine–coated slides using an Omnigrid arrayer (GeneMachines, San Carlos, CA).

Array Hybridization and Scanning. Ten nanograms each of tumor and reference DNA labeled with Cy5 and Cy3, respectively, were combined and briefly dried by Speedvac. The samples were resuspended in hybridization mix (50% formamide, 10% dextran sulfate, 3× SSC, 1.5% SDS) and heated to 70°C for 10 minutes, followed by 1-hour incubation at 37°C to allow blocking of repetitive sequences by human Cot-1 DNA. After incubation, samples were applied to the microarray under a coverslip and hybridized at 37°C for 18 hours. After hybridization, the arrays were then washed in 50% formamide and 2× SSC (pH 7.0) for 20 minutes at 45°C, followed by a 7-minute wash at room temperature in 0.1 mol/L $NaPO_4$ (pH 8.0) and 0.1% NP40. After washing, the arrays were dried by centrifugation at 600 rpm for 5 minutes.

Arrays were scanned with a GenePix 4000A scanner (Axon Instruments, Inc., Union City, CA); fluorescence data were processed with GenePix 3.0 image analysis software (Axon Instruments, Inc.). For each spot, $\log_2$ ratio = $\log_2(Cy5/Cy3)$ and average $\log_2$ intensity = $[\log_2(Cy5) + \log_2(Cy3)]/2$ were calculated, where Cy5 and Cy3 refer to the median foreground fluorescent signals of the tumor and reference DNA, respectively. Background subtraction was not used because it conferred no benefit in tests run on cell lines with varying numbers of X chromosome copies.[8] The $\log_2$ ratios on each array were normalized and corrected for intensity-based location adjustment with a block-level loess algorithm (32).

[4] Internet address: http://genome-www.stanford.edu/rap_sir/RNDA_B_amplification.shtml.

[5] Internet address: http://genome.ucsc.edu/.

[6] Internet address: http://www.fhcrc.org/labs/trask/arrayCGH.

[7] Internet address: http://bacpac.chori.org/.

[8] Unpublished results.

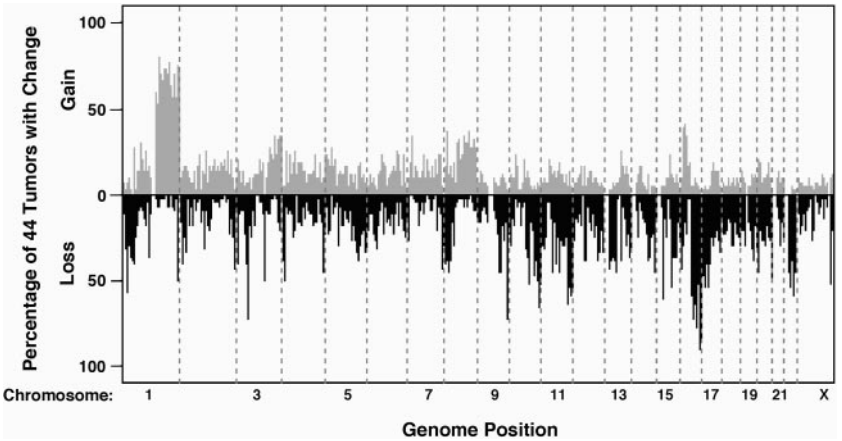

Fig. 1. Overall frequency of BAC copy number gain and loss for 44 breast tumors. The percentage of the 44 tumors showing gain (■; above 0) or loss (■; below 0) of DNA represented by each of the 4153 BACs is plotted against the corresponding genomic position of the BAC clone.

Bacterial Artificial Chromosome Array Quality Control and Preprocessing. The overall quality of the BAC array and the labeling method was established by hybridizing DNA samples from blood lymphocytes of each of 10 normal females *versus* a normal female reference, with labeling performed as described above (see Supplemental Data 1A). For all normal samples, 99% quantiles of the BAC clones were within $\log_2$ ratios of -0.175 to 0.154. The results were used to identify BAC clones producing inconsistent or unreliable hybridization results. BACs were excluded from the analysis if they exhibited one or more of the following characteristics consistently across the 10 normal *versus* normal arrays: large deviation from the expected $\log_2$ ratio value of 0, low spot intensity, or designation by the image analysis software as being of poor quality (*i.e.,* flagged spots). The analysis of 44 tumors was restricted to clones with no missing (flagged) values for any of the tumors.

Detection of Single Copy Number Changes with the BAC Array. To test the sensitivity and accuracy of the BAC array, we performed hybridizations of test DNA from cell lines containing one to five copies of the X chromosome (National Institute of General Medical Sciences Human Genetic Cell Repository, Camden, NJ) against normal female reference DNA (3, 5). Both test and reference samples were labeled by the PCR method described above. Parallel analyses were performed on sets of test DNA from fresh cultured cells and from cells processed to mimic the routine processing of tumor samples (cells harvested, centrifuged to a cell pellet, fixed in 10% buffered formalin, and embedded in paraffin before DNA extraction). For each sample, after normalization, the means of the 97 X-chromosome BACs and their SEs were calculated. These quantities were translated back to the ratio scale to directly examine the dose-response relationship between the estimated and underlying true X-chromosome copy numbers. Estimated ratios for both fixed and fresh samples are linearly related to the X-chromosome number with slopes of 0.239 ($R^2 = 0.99$) and 0.192 ($R^2 = 0.98$), respectively, compared with the ideal of 0.50 (Supplemental Data 1B). Error bars (95% confidence intervals) on the means are nonoverlapping for both fixed and fresh samples, showing that data from the BAC array can discriminate the differing numbers of X chromosomes. The underestimation of the magnitude of copy number deviations by array comparative genomic hybridization is consistent with that reported by others and is likely related to unsuppressed repeat sequences (3, 5).

Statistical Analysis. The two primary goals in this article were to (*a*) identify BACs or regions of BACs that differ in copy number between tumor subtypes and (*b*) examine correlations between BACs identified in the first goal and to explore whether any appear to act in conjunction in generating group differences. We first applied a categorical analysis to the BACs after classifying them as representing gain, loss, or no-change according to their $\log_2$ ratio values. Log_2 ratio values < -0.34 were categorized as losses, those > 0.38 as gains, and those in between as unchanged. These cutoff values were chosen to correspond to the mean $\log_2$ ratio values of the X-chromosome BACs from fixed cell lines containing 1X and 3X chromosomes, respectively, described in the previous section. These cutoffs should yield few false positive results. However, we may miss a few truly changed BACs. The counts of loss, gain, and no-change were summarized by tumor group for each BAC, providing 3×2 tables for analysis (3 categories $\times$ 2 tumor groups). Fisher's exact test was applied to these tables to test for a significant difference in the distribution of loss/gain/no-change between the tumor groups for each BAC. We used a permutation-based procedure of Westfall and Young (33) to adjust for multiple comparisons and denote these resulting *P* values as adjusted *P* values.

To increase our power for identifying regional changes in copy number between tumor subtypes, we averaged $\log_2$ ratios over windows of five consecutive BACs, sliding along the chromosome one BAC at a time. The average size of the window of five consecutive BACs was 3.55 Mb. A two-sample *t* statistic was used to compare the average $\log_2$ ratio for the tumor subtypes for each window. We computed adjusted *P* values with a modified permutation-based procedure of Westfall and Young [ref. 33; similar to that of Ge *et al.* (34)]. Because of the overlap in windows, we assigned to each BAC the smallest *P* value among the windows to which it belonged.

Both the single BAC and the 5-BAC window analyses were complementary to each other in detecting frequency differences between two tumor types. For focal changes (*i.e.,* changes that are only detected by single BACs), averaging over BACs within a window as in the 5-BAC window analysis could dilute the effect of the change at that locus. On the other hand, if the changes expand over a few BACs, averaging over those BACs will reduce the variance in frequency change, which will result in better power to detect smaller differences between the two groups than the single BAC analysis.

To explore how the BACs that differentiate between the tumor subtypes act jointly within each group, we conducted a correlation analysis. We used the standard Pearson correlation (henceforth referred to as correlation), which measures the magnitude and direction of the linear relationship between pairs of BACs to quantify whether they are changing in a concordant, discordant, or unrelated manner. The correlation analysis was performed for tumor subtypes, *e.g.,* ER positive and ER negative, by (*a*) choosing a subset of BACs to distinguish the subtypes (see following for specific criteria); (*b*) computing the pairwise correlation for all of the BACs from the subset, and (*c*) calculating *P* values for the correlations (while adjusting for multiple comparisons). Adjusted *P* values were obtained using a permutation-based procedure of Westfall and Young (33). BACs were selected in the first step, if either the difference in the BAC's gain or loss percentages between the tumor subtypes was $\geq$40% or if its adjusted *P* value from the categorical or windowed *t* statistic analysis was $\leq$0.30. These selection criteria were chosen to include BACs that may truly differ between tumor subtypes but did not achieve statistical significance because of insufficient power. It should be noted that this process of selecting BACs does not bias the correlation analysis because the selection is based on comparisons between tumor subtypes, whereas the correlations are computed within each subtype.

All analyses and cited *P* values have been adjusted for multiple comparisons. The analyses were performed in the open source statistical computing environment "R."[9]

RESULTS

Validation of DNA Labeling Method. To validate the PCR-based labeling method used, we compared it to random-primed labeling (6,

[9] Internet address: http://www.r-project.org.

7, 27) in samples of the X-chromosome cell lines that were either fresh or formalin-fixed (with the same procedure used to process the tumor samples). Both labeling methods were capable of detecting single copy changes on the X chromosome (data not shown). The PCR method produced greater BAC-to-BAC variability than the random-primed labeling, but it also resulted in larger mean differences between the copy number estimates. We also compared the array results from random-primed and PCR labeling for two of the archival tumors and found excellent correlation (correlation coefficients, 0.93 and 0.87, respectively; Supplemental Data 1C).

The array results for the archival tumors were highly reproducible: 12 of the archival tumors were relabeled by the PCR method and assayed in duplicate resulting in high correlation coefficients, ranging from 0.86 to 0.97 (data not shown). In addition, 5 of the 44 cases with high-level amplification events ($\log_2$ ratio $\geq$ 1.0) for overlapping BACs in 17q12 (containing the *c-erbB-2* gene) were also positive for overexpression of the c-erbB-2 protein. None of the low c-erbB-2 protein-expressing tumors showed amplification in those clones (data not shown).

Genomic Alterations in 44 Archival Breast Cancer Samples. We analyzed tumor DNA from 44 formalin-fixed breast cancer samples that had been dissected from paraffin-embedded blocks and flow-sorted to enrich for tumor cells. To identify overall trends across all of the tumors, we plotted the frequency of tumors showing gain or loss for each BAC across the genome (Fig. 1). We used the mean $\log_2$ ratios for the X-chromosome BACs obtained from the 3X (0.39) and 1X (−0.34) fixed cell lines in the X-chromosome titration experiment (see above) as our threshold for gain and loss, respectively. We observed a high frequency (≥30% of tumors) of regional (≥10 Mb) gains in 1q and losses in 1p36-p33, 5q31-q35, 8p21, 10q25-q26, 11q12-q13, 11q23-q25, 13q12-q14, 16q11-q24, 17p13-p11, and 22q11-q13 among these 44 breast tumors. In addition to the large regional alterations, the resolution of the BAC array allowed us to map smaller regions of gain or loss. In Supplemental Data 2, we indicate the chromosomal locations of the 411 BAC clones that showed gain or loss in ≥30% of the 44 tumors.

Genomic Alterations in Subtypes of Breast Cancer. On the basis of two distinguishing phenotypic characteristics, we characterized

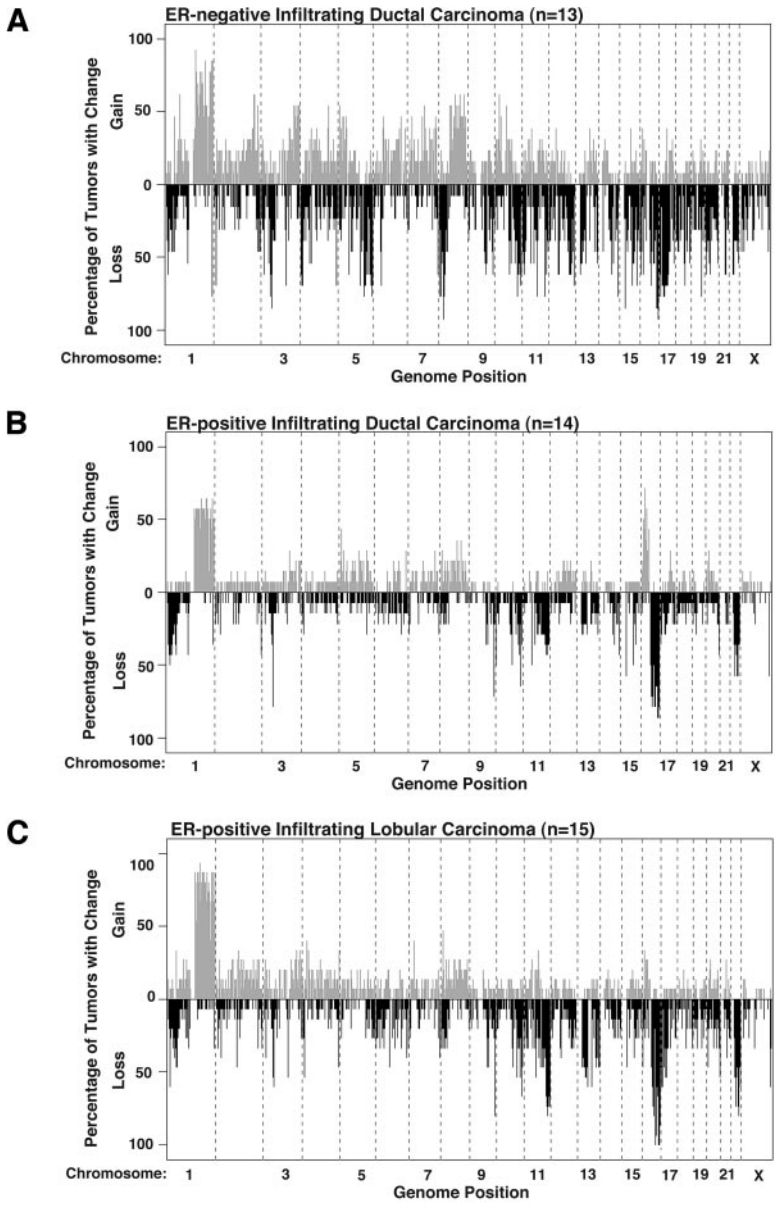

Fig. 2. Frequency of copy number gain and loss in subtypes of breast tumors. The percentage of copy number gain (■; above 0) and loss (■; below 0) were calculated for ER-negative infiltrating ductal carcinoma (*A*), ER-positive infiltrating ductal carcinoma (*B*), and ER-positive infiltrating lobular carcinoma (*C*).

genetic alterations that might be associated with subtypes of breast cancer. We compared three groups of tumors based on histology and ER status: (*a*) ER-negative infiltrating ductal carcinoma ($n = 13$); (*b*) ER-positive infiltrating ductal carcinoma ($n = 14$); and (*c*) ER-positive infiltrating lobular carcinoma ($n = 15$). The uncommon subtype ER-negative infiltrating lobular carcinoma tumors ($n = 2$) were not included in the analysis. Fig. 2 shows the frequency of BAC gain or loss within each of the three subtypes. We used four different approaches to identify BACs or groups of BACs that showed more frequent loss or gain in one subtype than another: (*a*) measurement of a difference in frequency of gain or loss between subtypes of ≥40%; (*b*) determination of significant difference in behavior of individual BACs between subtypes with Fisher's exact test; (*c*) determination of statistical difference between windows of five BACs with two-sample *t* statistic; and (*d*) observation of high-level loss and gain in ≥20% of tumors in each subtype.

Estrogen Receptor-negative *versus* Estrogen Receptor-positive Infiltrating Ductal Carcinomas. To identify genetic alterations that are associated with ER status in a single histologic type, we first compared the frequency of gains and losses in ER-negative and ER-positive infiltrating ductal carcinoma. The frequency of copy number changes in ER-negative infiltrating ductal carcinoma (8.7% of BACs showing gain in the subtype on average; 12.0% showing loss) was higher than in ER-positive infiltrating ductal carcinoma (3.9 and 5.8%, respectively). We observed that ER-negative infiltrating ductal carcinoma had ≥40% more frequent gains in 1p31, 1q23, 2q34, 2q36, 3q26-q28, 4q31, 5p14, 6p12, 6q24, 7q21, 8q21-q24, 10p12, and 10q21 and ≥40% more frequent losses in 1p13, 2p25, 3p25, 3p21, 3q21, 4p16, 4q35, 5q11, 5q22, 5q23, 5q31-q35, 6p21, 7q36, 8p23, 8p21, 8p12, 9q22, 10q22, 10q25-q26, 11p15, 11q13, 11q23, 12q13, 12q23-q24, 14q32, 15q25, 15q26, 16p13, 17p12-p11, 17q11.2-q12, 17q21, 18q21, 18q22, 19q13, 20p, 21q22, 22q11, and Xp22 than ER-positive infiltrating ductal carcinoma (Supplemental Data 2).

ER-positive infiltrating ductal carcinoma was primarily characterized by alterations in chromosome 16. As a group, they showed more frequent gains in 16p than ER-negative tumors, and most of chromosomal arm 16q showed more frequent losses in ER-positive than ER-negative infiltrating ductal carcinoma (Fig. 2).

Using Fisher's exact test to compare gain and loss of individual BACs between ER-negative and ER-positive infiltrating ductal carcinoma, we

Table 2 *BAC clones with significant frequency differences between ER-positive and ER-negative IDC subtypes or with high-level copy number changes in IDC and ILC subtypes of breast cancer*

BAC clone	Chromosome location	Adjusted *P* values for frequency differences between ER-positive and ER-negative IDC *	ER-positive IDC ($n = 14$)			ER-negative IDC ($n = 13$)			ER-positive ILC ($n = 15$)		
			No. with gain (%) †	No. with loss (%)	No. with high-level changes ‡	No. with gain (%)	No. with loss (%)	No. with high-level changes	No. with gain (%)	No. with loss (%)	No. with high-level changes
RP11-35C1	1q32		9 (64)	0 (0)		10 (77)	0 (0)		13 (87)	0 (0)	3 (G)
RP11-425J9	3p21		0 (0)	4 (29)		0 (0)	10 (77)	4 (L)	0 (0)	3 (20)	
RP11-82B23	3p21		0 (0)	11 (79)		0 (0)	10 (77)	3 (L)	0 (0)	9 (60)	
RP11-478C1 §	4p16	0.074	0 (0)	0 (0)		0 (0)	8 (62)		0 (0)	4 (27)	
RP11-17I9 §	4p16	0.013	0 (0)	0 (0)		0 (0)	9 (69)		0 (0)	1 (7)	
RP11-89G4 §	5q23	0.002	0 (0)	0 (0)		0 (0)	10 (77)		0 (0)	1 (7)	
CTD-2090L24 §	5q31	0.074	0 (0)	0 (0)		0 (0)	8 (62)		1 (7)	0 (0)	
RP11-81D21 §	5q31	0.035	1 (7)	0 (0)		0 (0)	9 (69)		0 (0)	0 (0)	
RP11-507E2	5q33		0 (0)	1 (7)		0 (0)	8 (62)	3 (L)	0 (0)	3 (20)	
RP11-14K9 §	5q35	0.061	1 (7)	0 (0)		1 (8)	8 (62)		1 (7)	0 (0)	
RP11-69A18 §	5q35	0.013	0 (0)	0 (0)		1 (8)	8 (62)		0 (0)	2 (13)	
CTD-2129M9 §	5q35	0.013	0 (0)	0 (0)		1 (8)	8 (62)		0 (0)	3 (20)	
RP11-105L4 §	5q35	0.013	0 (0)	0 (0)		0 (0)	9 (69)		0 (0)	2 (13)	
RP11-564G9 §	5q35	0.012	0 (0)	1 (7)		1 (8)	10 (77)		0 (0)	3 (20)	
RP11-2I16 §	5q35	0.012	1 (7)	0 (0)		1 (8)	9 (69)		0 (0)	2 (13)	
RP1-240G13 §	5q35	0.071	0 (0)	1 (7)		1 (8)	9 (69)		0 (0)	4 (27)	
RP11-86A14 §	8p23	0.037	0 (0)	1 (7)		0 (0)	10 (77)		0 (0)	4 (27)	
RP11-240A17 §	8p23	0.037	0 (0)	1 (7)		0 (0)	10 (77)		0 (0)	3 (20)	
RP11-82K8 §	8p23	0.037	0 (0)	1 (7)		0 (0)	10 (77)		0 (0)	5 (33)	
RP11-112G9	8p23		4 (29)	0 (0)		3 (23)	2 (15)	3 (G)	7 (47)	1 (7)	3 (G)
RP11-235I5	8p23		0 (0)	2 (14)		0 (0)	10 (77)	3 (L)	0 (0)	5 (33)	
RP11-459E5 §	8p21	0.037	0 (0)	3 (21)		0 (0)	12 (92)	5 (L)	0 (0)	4 (27)	
RP11-237F24	8q24		3 (21)	0 (0)		8 (62)	0 (0)	4 (G)	2 (13)	0 (0)	
RP11-158G1	8q24		1 (7)	0 (0)		5 (38)	2 (15)	3 (G)	3 (20)	0 (0)	
RP11-43K6 §	10p12	0.074	0 (0)	0 (0)		8 (62)	0 (0)		2 (13)	0 (0)	
RP11-46G13 §	10q25	0.037	0 (0)	1 (7)		0 (0)	10 (77)		0 (0)	4 (27)	
RP11-98G24	11q13		2 (14)	0 (0)		0 (0)	0 (0)		3 (20)	1 (7)	3 (G)
RP11-31F2	11q13		1 (7)	0 (0)		0 (0)	0 (0)		3 (20)	1 (7)	3 (G)
RP11-79B7	11q14		1 (7)	0 (0)		0 (0)	0 (0)		3 (20)	1 (7)	3 (G)
RP11-109J21	16q12		0 (0)	11 (79)	3 (L)	0 (0)	7 (54)		0 (0)	11 (73)	
RP11-280N16	16q23		0 (0)	10 (71)		0 (0)	9 (69)		0 (0)	14 (93)	3 (L)
RP11-442O1	16q24		0 (0)	12 (86)		0 (0)	11 (85)		0 (0)	15 (100)	3 (L)
RP11-542M13	16q24		0 (0)	12 (86)	3 (L)	0 (0)	11 (85)	3 (L)	0 (0)	15 (100)	5 (L)
RP11-160E2 §	17p11	0.013	0 (0)	0 (0)		0 (0)	9 (69)		0 (0)	2 (13)	
RP11-62N23	17q21		0 (0)	1 (7)		5 (38)	0 (0)	4 (G)	0 (0)	0 (0)	
CTD-2019C10	17q21		0 (0)	0 (0)		5 (38)	0 (0)	4 (G)	0 (0)	0 (0)	
RP11-94L15	17q21		0 (0)	0 (0)		5 (38)	0 (0)	4 (G)	0 (0)	0 (0)	
RP11-387H17	17q21		0 (0)	0 (0)		3 (23)	0 (0)	4 (G)	0 (0)	0 (0)	
RP11-749I16	17q21		0 (0)	0 (0)		3 (23)	1 (8)	3 (G)	0 (0)	0 (0)	
RP11-317E13	19q13		0 (0)	1 (7)		0 (0)	8 (62)	3 (L)	0 (0)	4 (27)	
RP11-208I3 §	19q13	0.074	0 (0)	0 (0)		0 (0)	8 (62)		0 (0)	0 (0)	
RP11-79D9 §	21q22	0.074	0 (0)	0 (0)		0 (0)	8 (62)		0 (0)	3 (20)	

NOTE

* *P* values from Fisher's exact test on categorized $\log_2$ ratio values.

† Categories were gain, loss, or no change.

‡ $\log_2$ ratio ≥ 1.0 categorized as high-level gain (G); $\log_2$ ratio ≤ −1.0 categorized as homozygous loss (L).

§ BACs with adjusted *P* values ≤ 0.10.

Abbreviations: ILC, infiltrating lobular carcinoma; IDC, infiltrating ductal carcinoma.

identified 14 BACs that were significantly different between the two subtypes (adjusted P values ≤ 0.05), including losses in 4p16, 5q23, 5q31, 5q35, 8p23, 8p21, 10q25, and 17p11.2. Using a somewhat less conservative level of significance (adjusted $P \leq 0.10$) to account for the adjustment of the P for multiple comparisons, we identified an additional seven BACs that were different between the two subtypes (losses in 19q13 and 21q22 and gain in 10p12; Table 2). The bold lines on Fig. 3 indicate the location of the 21 BACs showing differences between ER-negative and ER-positive infiltrating ductal carcinoma with this test. As seen in the figure, the BACs achieving a level of significance with Fisher's exact test are often part of larger regions that differ in frequency of loss and gain between the two groups.

To additionally assess copy number gains or losses larger than those defined by single BACs, we applied a two-sample t statistic comparing a sliding window of five consecutive BAC clones in the subtypes. Using this test, we observed differences between ER-negative and ER-positive infiltrating ductal carcinoma for BACs at the following locations: 2p16-p14, 5q31, and 6p22 (P values ≤ 0.05) and 10q11-q21 (P values ≤ 0.10). There was suggestive evidence of differences in 1p31, 2q34, 5q23, 5q32-q33, 8p23-p22, 8p21, 10p12, 11q22, and 17q21 (P values ≤ 0.20 for at least one of the BACs in the region). Supplemental Data 2 details the domains of the regions that exhibit differences in frequency of copy number gain and loss between the two subtypes based on this analysis. There were several regions (*e.g.,* 5q23-31, 8p23, 8p21, and 10p12) identified as significant (or close to) for both individual BAC and 5-BAC window analyses between ER-negative and ER-positive infiltrating ductal carcinoma.

We also compared the subtypes for the frequency with which particular BACs showed high-level amplifications ($\log_2$ ratio ≥ 1.0; approximately six copies assuming a modal diploid genome) or apparent homozygous deletions ($\log_2$ ratio ≤ -1.0; no copies, assuming a modal diploid genome). BAC clones showing such deviations in at least 20% of the tumors in a subtype are indicated by triangles on Fig. 3. Table 2 details the BACs with high-level alterations. Overall, ER-negative infiltrating ductal carcinoma had more high-level amplifications and apparent homozygous deletions than ER-positive infiltrating ductal carcinoma. We observed high-level amplifications in ER-negative infiltrating ductal carcinoma at 8p23, 8q24, and 17q21 and no high-level amplifications in ER-positive infiltrating ductal carcinoma. Four of the 13 ER-negative tumors (31%) exhibited a high-level gain of BAC RP11-237F24 (8q24), which contains the proto-oncogene *c-myc*. A similarly frequent high-level gain was seen in 31% of ER-negative infiltrating ductal carcinoma for a series of overlapping BAC clones in 17q21 that contain the *c-erbB-2* gene and several other genes involved in tumorigenesis.

Several apparent homozygous deletions that contain putative tumor suppressors were observed in ER-negative infiltrating ductal carcinoma. These include regions in 3p21, 5q33, 8p23, 8p21, 9q34, 16q24, and 19q13 (Table 2; Supplemental Data 2). In ER-positive infiltrating ductal carcinoma, we detected the appearance of homozygous deletions in only two regions: 16q12 and 16q24. Loss of BACs in 16q24 was also observed in a similar fraction of ER-negative tumors.

Estrogen Receptor-positive Infiltrating Ductal Carcinoma *versus* Estrogen Receptor-positive Infiltrating Lobular Carcinoma. To identify regions of loss and gain associated with histologic type, we compared the frequencies of genetic alterations between ER-positive infiltrating ductal carcinoma and infiltrating lobular carcinoma tumors. Interestingly, ER-positive infiltrating lobular carcinoma had a slightly higher overall frequency of gain (5.2% of BACs on average) and loss (8.2% of BACs on average) throughout the genome than ER-positive infiltrating ductal carcinoma (3.9 and 5.8%, respectively). Both histologic types showed a high frequency of gain in 1q. However, gains in that chromosomal arm were more frequently seen in infiltrating lobular carcinoma ($\geq$40% difference between infiltrating lobular carcinoma and infiltrating ductal carcinoma tumors; see Supplemental Data 2). Infiltrating lobular carcinoma also showed more frequent losses in 11q and 16p than infiltrating ductal carcinoma. No BACs showed a statistically significant difference of gain or loss with Fisher's exact test or with the two-sample t statistic comparing a sliding window of five consecutive BACs. High-level amplification and apparent homozygous deletion events were more frequent in infiltrating

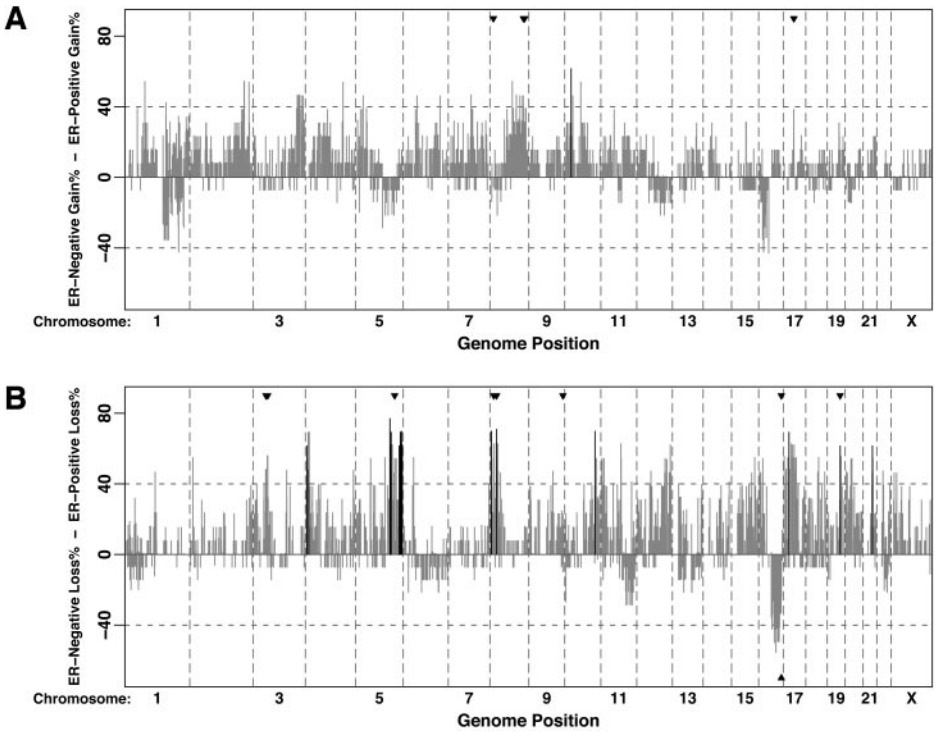

Fig. 3. Difference of gain and loss of BACs between ER-negative and ER-positive IDC tumors. *A*. This panel shows the percent difference of gain determined by subtracting the percent of ER-positive tumors showing gain from the ER-negative tumors showing gain. *B*. The difference in loss at individual BACs between the two subtypes was similarly determined. ■ indicates those BACs that showed differences between the subtypes by Fisher's exact test ($P \leq 0.10$). ▼ indicates the location of BACs that showed high-level gain ($\log_2$ ratio ≥ 1.0) or apparent homozygous deletion ($\log_2$ ratio < -1.0) in $\geq$20% of ER-negative (*top border*) or ER-positive (*bottom border*) tumors.

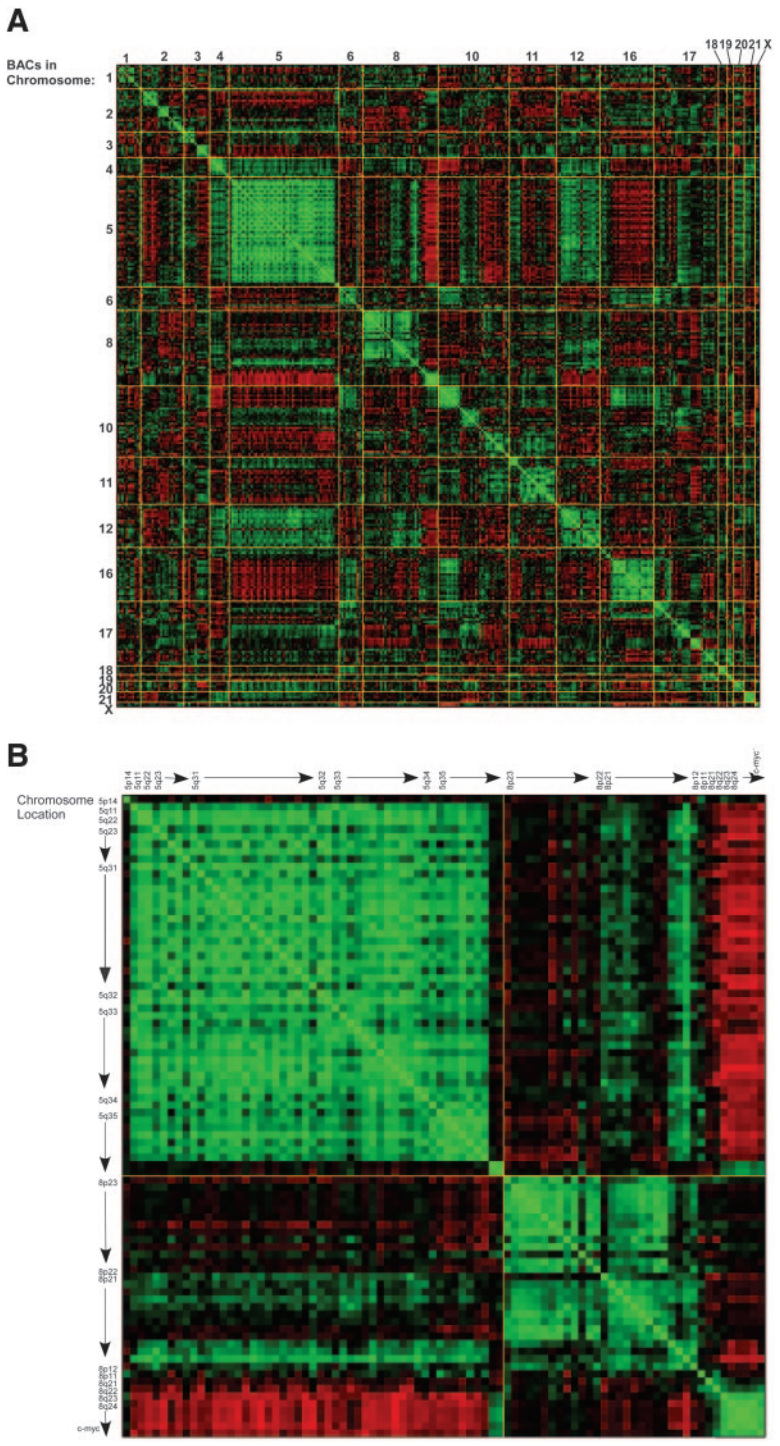

Fig. 4. Correlation matrix of copy number changes for ER-negative infiltrating ductal carcinoma tumors. *A*. The heat maps show positive (change in same direction; *green*) and negative (change in opposite direction; *red*) correlation between loss or gain of individual BACs for the 13 ER-negative infiltrating ductal carcinoma tumors. The 307 BACs that showed frequent change in ER-negative tumors are shown in genome order (see Supplemental Data 3 for complete list of BACs included in the correlation analysis). Because so few BACS on chromosomes 7, 9, 13, 14, 15, and 22 exhibited change in the ER-negative tumors, these chromosomes are not shown on the matrix. *B*. The heat map of correlations between chromosomes 5 and 8 is expanded. Chromosomal band information is designated. In the expanded view, BACs showing correlation between 5q loss and 8p21 loss and correlation between 5q loss and 8q24 gain are evident.

lobular carcinoma compared with infiltrating ductal carcinoma (Table 2).

Correlation of Loss or Gain Changes in Estrogen Receptor-negative Infiltrating Ductal Carcinoma Tumors. ER-negative tumors exhibited the highest frequency of copy number change among the subtypes. Pairwise correlation analysis of the subset of ER-negative tumors, including 307 BACs that exhibited frequent loss or gain in ER-negative tumors (Supplemental Data 3), revealed chromosomal alterations that coexist in this group of tumors. The heat maps in Fig. 4 show regions of positive (change in same direction: green) and negative (change in opposite direction: red) correlations between certain BACs. In all, 121 BAC combinations showed correlation coefficients ≥ 0.80 (data not shown). Relatively large regions of correlation were seen between changes in copy number of BACs on chromosome 5q and chromosomes 8, 10, 11, 12, 16, 17, and 20. There was correlation between loss in 5q33-q35 and (*a*) loss in 8p21 and 12q24 and (*b*) gain in 10p12. Loss of seven BACs from chromosome 5q showed correlation (coefficients of < -0.80) with copy number gain in the BAC encompassing the *c-myc* oncogene in 8q24 (Fig. 4*B*).

DISCUSSION

In this study, we used high-resolution array comparative genomic hybridization to evaluate copy number changes in archival breast

cancers. We also examined differences in genomic alterations between important phenotypic subtypes of breast cancer. Although the archival nature of tumor samples presents challenges to evaluation with array comparative genomic hybridization, we show that it is feasible to perform array comparative genomic hybridization with relatively small amounts of DNA from fixed samples.

On the basis of the analysis of the 44 breast tumors, we observed large regional gains in 1q, 3q, 8q, and 16p and losses in 1p, 3p, 5q, 8p, 9q, 10q, 11q, 13q, 16q, 17p, and 22q, many of which have been reported by previous studies with conventional comparative genomic hybridization methods (1, 2, 35–38). Our ability to identify a high frequency of loss in these samples in likely due to the flow-sorting step used to enrich tumor cells, which removed normal cells that could mask the presence of loss. Gain in 20q, reported in some conventional comparative genomic hybridization studies, was not apparent in this set of tumors. As has been reported in other studies, including those done by array comparative genomic hybridization, gain in 1q and loss in 16q were frequent alterations common to all types of breast tumors (1, 2, 37, 39). Interestingly, analysis of subtypes in our study revealed a higher frequency of gain in regions of 1q and loss in 16q11-q23 for ER-positive infiltrating ductal carcinoma compared with ER-negative infiltrating ductal carcinoma. This pattern of loss has also been seen in lobular and low-grade breast cancers by others and might indicate rearrangements involving the pericentromeric regions of chromosomes 1 and 16 (2, 37, 40). Our data support the idea that copy number changes in 1q and 16q are critical and early events in the initiation of breast cancer and that these changes may be particularly associated with the development of ER-positive disease.

The phenotypic subtypes we examined, based on ER status and histologic type, are of major clinical and biological importance. ER-negative tumors are more likely to occur in premenopausal women, in African-American women, and in women who carry a BRCA1 hereditary mutation (41, 42), and it is therefore possible that this phenotype results from alterations in specific biological pathways. Using the frequency of high-level amplifications and deletions and relatively conservative statistical methods to highlight BACs and regions that differed significantly between the ER subtypes, we found several regions of change more frequently associated with ER-negative infiltrating ductal carcinoma than ER-positive infiltrating ductal carcinoma. Notably, several of the BACs that showed a greater frequency of loss in ER-negative infiltrating ductal carcinoma cover regions containing genes that encode proteins central to sensing and repairing DNA damage, including *RAD50* (5q23), *FANCC* (9q22) and *FANCD2* (3p25), and *CHEK2* (22q12) (43, 44). In addition, a *BRCA1* modifier locus for hereditary breast cancer resides in the 5q region of loss we associated with ER-negative disease (45), indicating another possible link between loss in this region and defects in the repair of double-stranded DNA breaks.

In addition, this study highlights regions of interest that differentiate ER-negative infiltrating ductal carcinoma and ER-positive infiltrating ductal carcinoma. For example, the recent identification of allelic loss in 5q in association with a basal-like subclass of breast cancers (46) correlates with the 5q loss we found in ER-negative infiltrating ductal carcinoma. A relationship between amplification of oncogenes *c-erbB-2* and *c-myc* in ER-negative disease was also seen in this set of breast cancers. The amplicon in 8q24 containing *c-myc* and the amplicon in 17q12 containing *c-erbB-2* and several other potential oncogenes (47) were restricted to ER-negative infiltrating ductal carcinoma tumors.

As with ER status, histologic subtype is a major division of breast tumors associated with differences in etiology and clinical behavior (48). The regions of copy number change associated with infiltrating lobular carcinoma in our analysis are consistent with those previously reported, particularly the frequent losses in 16q (2, 24). Unlike most studies that find a higher rate of copy number changes in infiltrating ductal carcinoma compared with infiltrating lobular carcinoma (2, 13), we found a higher overall frequency of genomic change in ER-positive infiltrating lobular carcinoma than infiltrating ductal carcinoma (Fig. 2). This is most likely due to the difference in comparison groups: other studies compare infiltrating lobular carcinoma to infiltrating ductal carcinoma without regard to ER status, whereas our study compared ER-positive infiltrating lobular carcinoma to ER-positive infiltrating ductal carcinoma.

When we compared the frequency of gains and losses in ER-positive infiltrating ductal carcinoma and infiltrating lobular carcinoma, no BACs differentiated the groups with statistical significance with Fisher's exact test. However, at least 40% more ER-positive infiltrating lobular carcinoma tumors showed gains in 1q31-q32 and losses in 11q23-q25 than did ER-positive infiltrating ductal carcinoma (Supplemental Data 2). The identification of high-level amplifications and homozygous deletions in ER-positive infiltrating ductal carcinoma and infiltrating lobular carcinoma revealed three regions that differentiated infiltrating lobular carcinoma. In one region, the amplification in 11q13, has been identified in breast cancer (49) but has not been previously associated with lobular cancer.

Undoubtedly, genetic events at different genomic regions act concordantly in cancer development. To begin the process of identifying regions of chromosomal loss and gain that commonly coexist in breast cancers, we performed correlation analysis between BACs frequently changed in the tumors. Although our analysis in a relatively small set of tumors only begins to address the possible combinations of cooperating regions, trends of correlation between chromosomal regions were observed. The heat map in Fig. 4 shows regions of correlation between loss and gain in small and large chromosomal regions. These exploratory analyses provide new insights into gene-gene interactions in specific subtypes of breast cancers. Larger studies will provide sufficient power to identify regions that act synergistically to promote tumor progression. The application of targeted higher resolution arrays (11), along with complementary studies of allelic loss, methylation, and mutation, will also help additionally define the relevant changes in these important breast cancer subtypes.

ACKNOWLEDGMENTS

We thank Stephanie Stafford and Ann Yoder for database support, Julie Bittner for tissue procurement support, and Kelly Wirtala and Angela Chang for technical contributions.

REFERENCES

1. Tirkkonin M, Tanner M, Karhu R, Kallioniemi A, Isola J, Kallioniemi O-P. Molecular cytogenetics of primary breast cancer by CGH. Genes Chromosomes Cancer 1998; 21:177–84.
2. Richard F, Pacyna-Gengelbach M, Schluns K, et al. Patterns of chromosomal imbalances in invasive breast cancer. Int J Cancer 2000;89:305–10.
3. Pinkel D, Segraves R, Sudar D, et al. High resolution analysis of DNA copy number variation using comparative genomic hybridization to microarrays. Nat Genet 1998; 20:207–11.
4. Albertson DG. Profiling breast cancer by array CGH. Breast Cancer Res Treat 2003;78:289–98.
5. Snijders AM, Nowak N, Segraves R, et al. Assembly of microarrays for genome-wide measurement of DNA copy number. Nat Genet 2001;29:263–4.
6. Pollack J, Perou C, Alizadeh A, et al. Genome-wide analysis of DNA copy-number changes using cDNA microarrays. Nat Genet 1999;23:41–6.
7. Paris P, Albertson D, Alers J, et al. High-resolution analysis of paraffin-embedded and formalin-fixed prostate tumors using comparative genomic hybridization to genomic microarrays. Am J Pathol 2003;162:763–70.
8. van Dekken H, Paris P, Albertson D, et al. Evaluation of genetic patterns in different tumor areas of intermediate-grade prostatic adenocarcinomas by high-resolution genomic array analysis. Genes Chromosomes Cancer 2004;39:249–56.

9. Veltman J, Fridlyand J, Pejavar S, et al. Array-based comparative genomic hybridization for genome-wide screening of DNA copy number in bladder tumors. Cancer Res 2003;63:2872–80.
10. Weiss M, Kuipers E, Postma C, et al. Genomic profiling of gastric cancer predicts lymph node status and survival. Oncogene 2003;22:1872–9.
11. Ishkanian A, Malloff C, Watson S, et al. A tiling resolution DNA microarray with complete coverage of the human genome. Nat Genet 2004;36:299–303.
12. Persson K, Pandis N, Mertens F, et al. Chromosomal aberrations in breast cancer: a comparison between cytogenetics and comparative genomic hybridization. Genes Chromosomes Cancer 1999;25:115–22.
13. Nishizaki T, Chew K, Chu L, et al. Genetic alterations in lobular breast cancer by comparative genomic hybridization. Int J Cancer 1997;74:513–7.
14. Kallioniemi A, Kallioniemi OP, Sudar D, et al. Comparative genomic hybridization for molecular cytogenetic analysis of solid tumors. Science (Wash. DC) 1992;258: 818–21.
15. Muleris M, Almeida A, Gerbault-Seureau M, Malfoy B, Dutrillaux B. Detection of DNA amplification in 17 primary breast carcinomas with homogeneously staining regions by a modified comparative genomic hybridization technique. Genes Chromosomes Cancer 1994;10:160–70.
16. Isola JJ, Kallioniemi OP, Chu LW, et al. Genetic aberrations detected by comparative genomic hybridization predict outcome in node-negative breast cancer. Am J Pathol 1995;147:905–11.
17. Lisitsyn N, Lisitsina N, Dalbagni G, et al. Comparative genomic analysis of tumors: detection of DNA losses and amplification. Proc Natl Acad Sci USA 1995;92:151–5.
18. Courjal F, Theillet C. Comparative genomic hybridization analysis of breast tumors with predetermined profiles of DNA amplification. Cancer Res 1997;57:4368–77.
19. Clark G. Prognostic and predictive factors. In: Harris J, editor. Diseases of the breast, Vol. 2. Philadelphia: Lippincott, Williams & Wilkins; 2000. p. 489–514.
20. Perou C, Serlie T, Eisen M, et al. Molecular portraits of human breast tumors. Nature (Lond.) 2000;406:747–52.
21. Stierer M, Rosen H, Weber R, Hanak H, Spona J, Tuchler H. Immunohistochemical and biochemical measurement of estrogen and progesterone receptors in primary breast cancer: correlation of histopathology and prognostic factors. Ann Surg 1993; 218:13–21.
22. Harris M, Howell A, Chrissohou M, Swindell RI, Hudson M, Sellwood RA. A comparison of the metastatic pattern of infiltrating lobular carcinoma and infiltrating duct carcinoma of the breast. Br J Cancer 1984;50:23–30.
23. Berx G, Van Roy F. The E-cadherin/catenin complex: an important gatekeeper in breast cancer tumorigenesis and malignant progression. Breast Cancer Res 2001;3: 289–93. Epub 2001 Jun 28.
24. Gunther K, Merkelbach-Bruse S, Amo-Takyi BK, Handt S, Schroder W, Tietze L. Differences in genetic alterations between primary lobular and ductal breast cancers detected by comparative genomic hybridization. J Pathol 2001;193:40–7.
25. Glogovac J, Porter P, Banker D, Rabinovich P. Cytokeratin labeling of breast cancer cells extracted from paraffin embedded tissue for bivariate flow cytometric analysis. Cytometry 1996;24:260–7.
26. Frank T, Svoboda-Newman S, Hsi E. Comparison of methods for extracting DNA from formalin-fixed paraffin sections for nonisotopic PCR. Diagn Mol Pathol 1996; 5:220–4.
27. Lieb J, Liu X, Botstein D, Brown P. Promoter-specific binding of Rap1 revealed by genome-wide maps of protein-DNA association. [comment][erratum appears in Nat Genet 2001;29:100]. Nat Genet 2001;28:327–34.
28. Cheung V, Nowak N, Jang W, et al. Integration of cytogenetic landmarks into the draft sequence of the human genome. Nature (Lond.) 2001;409:953–8.
29. Knight SJ, Lese CM, Precht KS, et al. An optimized set of human telomere clones for studying telomere integrity and architecture. Am J Hum Genet 2000;67:320–32.
30. Kent W, Sugnet C, Furey T, et al. The human genome browser at UCSC. Genome Res 2002;12:996–1006.
31. Klein C, Schmidt-Kittler O, Schardt J, Pantel K, Speicher M, Riethmuller G. Comparative genomic hybridization, loss of heterozygosity, and DNA sequence analysis of single cells. Proc Natl Acad Sci USA 1999;96:4494–9.
32. Yang YH, Dudoit S, Luu P. Speed TP. Normalization for cDNA microarray. In: Bittner ML, Chen Y, Dorsel AN, Dougherty ER, editors. Microarrays: optical technologies and informatics. Bellingham, WA: SPIE, Society for Optical Engineering; 2001. p. 141–52.
33. Westfall PH, Young SS. Resampling-based multiple testing: examples and methods for P-value adjustment. New York: John Wiley and Sons; 1993.
34. Ge Y, Dudoit S, Speed TP. Resampling-based testing for microarray data analysis. Test 2003;12:1–77.
35. Kallioniemi OP, Kallioniemi A, Piper J, et al. Optimizing comparative genomic hybridization for analysis of DNA sequence copy number changes in solid tumors. Genes Chromosomes Cancer 1994;10:231–43.
36. Buerger H, Otterbach F, Simon R, et al. Comparative genomic hybridization of ductal carcinoma *in situ* of the breast: evidence of multiple genetic pathways. J Pathol 1999;187:396–402.
37. Cingoz S, Altungoz O, Canda T, Saydam S, Aksakoglu G, Sakizli M. DNA copy number changes detected by comparative genomic hybridization and their association with clinicopathologic parameters in breast tumors. Cancer Genet Cytogenet 2003; 145:108–14.
38. Roylance R, Gorman P, Harris W, et al. Comparative genomic hybridization of breast tumors stratified by histological grade reveals new insights into the biological progression of breast cancer. Cancer Res 1999;59:1433–6.
39. Pollack J, Sorlie T, Perou C, et al. Microarray analysis reveals a major direct role of DNA copy number alteration in the transcriptional program of human breast tumors. Proc Natl Acad Sci USA 2002;99:12963–8.
40. Pandis N, Heim S, Bardi G, Idvall I, Mandahl N, Mitelman F. Whole-arm t(1;16) and i(1q) as sole anomalies identify gain of 1q as a primary chromosomal abnormality in breast cancer. Genes Chromosomes Cancer 1992;5:235–8.
41. Anderson W, Chatterjee N, Ershler W, Brawley O. Estrogen receptor breast cancer phenotypes in the Surveillance, Epidemiology, and End Results database. Breast Cancer Res Treat 2002;76:27–36.
42. Lakhani S, van de Vijver M, Jacquemier J, et al. The pathology of familial breast cancer: predictive value of immunohistochemical markers estrogen receptor, progesterone receptor, HER-2, and p53 in patients with mutations in BRCA1 and BRCA2. J Clin Oncol 2002;20:2310–8.
43. Zhou BB, Elledge SJ. The DNA damage response: putting checkpoints in perspective. Nature (Lond.) 2000;408:433–9.
44. Garcia-Higuera I, Taniguchi T, Ganesan S, et al. Interaction of the Fanconi anemia proteins and BRCA1 in a common pathway. Mol Cell 2001;7:249–62.
45. Nathanson K, Shugart Y, Omaruddin R, et al. CGH-targeted linkage analysis reveals a possible BRCA1 modifier locus on chromosome 5q. Hum Mol Genet 2002;11: 1327–32.
46. Wang Z, Lin M, Wei L-J, et al. Loss of heterozygosity and its correlation with expression profiles in subclasses of invasive breast cancer. Cancer Res 2004;64:64–71.
47. Kauraniemi P, Barlund M, Monni O, Kallioniemi A. New amplified and highly expressed genes discovered in the ERBB2 amplicon in breast cancer by cDNA microarrays. Cancer Res 2001;61:8235–40.
48. Harris J, Lippman M, Veronesi U, Willit W. Breast cancer (1). N Engl J Med 1992;327:319–28.
49. Schuuring E, Verhoeven E, van Tinteren H, et al. Amplification of genes within the chromosome 11q13 region is indicative of poor prognosis in patients with operable breast cancer. Cancer Res 1992;52:5229–34.

Array Comparative Genomic Hybridization Analysis of Genomic Alterations in Breast Cancer Subtypes

Lenora W. M. Loo, Douglas I. Grove, Eleanor M. Williams, et al.

Cancer Res 2004;64:8541-8549.